Advances in Science and Technology Research Journal

Advances in Science and Technology Research Journal, 2026, 20(4), 91–104
https://doi.org/10.12913/22998624/214300
ISSN 2299-8624, License CC-BY 4.0

Received: 2025.10.03
Accepted: 2026.02.15
Published: 2026.03.01

Comparative study on high-temperature embrittlement of duplex stainless steels

Jerzy Łabanowski[1*], Santina Topolska[2]

[1] Institute of Manufacturing and Materials Technology, Faculty of Mechanical Engineering and Ship Technology, Gdańsk University of Technology, ul. Gabriela Narutowicza 11/12, 80-233, Gdańsk, Poland
[2] Department of Welding Engineering, Faculty of Mechanical Engineering, Silesian University of Technology, ul. Konarskiego 18a, 44-100 Gliwice, Poland
* Corresponding author's e-mail: jlabanow@pg.edu.pl

ABSTRACT

The aim of this article was to investigate the impact of ageing heat treatment of 2101 lean duplex steel on changes in the microstructure and mechanical properties, mainly impact toughness. Steel was subjected to ageing treatments in the temperature range of 500–900 °C with exposure times of 1, 10, and 100 hours. Light microscope examinations, hardness measurements and impact toughness tests were performed. The obtained results confirm that high-temperature service of duplex stainless steels should be avoided. Precipitation of secondary phases (mainly α', σ, γ_2 phases) strongly deteriorates mechanical properties of steels but some amounts of these phases may be acceptable in the microstructure depending upon the application of the steel. The test results obtained for 2101 lean duplex steel were compared with the results obtained earlier for higher alloy 2205 and 2507 duplex steel grades. The research showed that the loss of plasticity after ageing at 500 °C affects the 2101 lean duplex steel the most, while ageing at higher temperatures, above 700 °C, limits the plasticity of 2205 and 2507 steel grades to a much greater extent.

Keywords: duplex stainless steels; lean duplex steel; heat treatment; embrittlement, operating temperature.

INTRODUCTION

Stainless steels are an important group of structural materials widely used across numerous industrial sectors, including chemical, food and beverage, energy and power generation, petrochemical, pulp and paper, medical, automotive, aerospace, and marine industries [1–3]. They comprise four principal groups: ferritic, martensitic, austenitic, and duplex stainless steels [4–7]. Among them, steels with a ferritic and austenitic structure, characterized by an almost equal volume fraction of both phases, hold a particularly prominent position [8–10]. Duplex steel products are delivered after solution annealing heat treatment [11]. The solution temperature should ensure the desired ratio of the amount of ferrite and austenite phases in the microstructure, as well as the appropriate chemical composition of these phases, which is important from the point of view of corrosion resistance [12]. Solution annealing should be performed at a temperature high enough to dissolve all precipitates of intermetallic phases. The recommended heat treatment temperature is in the range of 1040–1100 °C (depending on the steel grade). Quenching from these temperatures gives an optimal microstructure and avoids precipitation processes during cooling.

Secondary thermal cycles may lead to destabilization of primary phases, as a result of which new and often undesirable components may be formed in the structure, such as secondary solutions (secondary austenite), carbides, carbonitrides and other intermetallic phases [13–15]. In the temperature range of 650–950 °C, there is a risk of precipitation of carbides and intermetallic phases (mainly the σ phase), which make the steel brittle and reduce its corrosion resistance. The presence of 1–2% of the σ phase in the structure can reduce the impact toughness of steel by half, while if the share of this phase exceeds 5%,

there is a sharp decrease in corrosion resistance and practically loss of plasticity [16].

In the temperature range of 300–550 °C the phenomenon of so-called "475 °C embrittlement" occurs [17]. It is spinodal decomposition in the ferritic phase leading to change in the microstructure and release of the chromium-rich α' phase, which also results in a significant reduction in the ductility of steel. A schematic time-temperature-precipitation (TTP) chart indicating the temperature ranges for the release of secondary phases in duplex steels is shown in Figure 1. This graph shows the influence of various alloying elements on the beginning of the transformation and it's temperature range [18]. Higher contents of Cr, Mo, W, Si in the chemical composition of steel increase the range of stability of intermetallic phases and shift the nose of the TTP curves towards shorter initiation times of precipitation processes. This mechanism clearly indicates that steels with a higher content of alloying elements such as super duplex or hyper duplex will show a greater tendency to precipitation processes at elevated temperatures. Transformations resulting in the appearance of intermetallic phases mainly concern ferrite due to the fact that the rate of diffusion of alloying elements in this phase is about two orders of magnitude higher than in austenite. Ferrite is enriched in Cr and Mo, i.e. elements that constitute the basis of intermetallic phases [19]. The low temperature at the beginning of precipitation processes excludes the use of duplex steel for operation at temperatures above 280 °C [20].

An isothermal precipitation diagram for 2304, 2205, and 2507 duplex stainless steels is shown in Figure 2. The start of chromium carbide and nitride precipitation begins at the relatively slow time of 1–2 minutes at temperature. This is slower than in the ferritic grades or the highly alloyed austenitic grades, and is due, to the high solubility of carbon and nitrogen in the low nickel austenite phase and possibly to a retardation effect of nitrogen on the carbide precipitation. The carbide and nitride formation kinetics are slightly affected by chromium, molybdenum, and nickel, so all the nitrogen-alloyed duplex stainless steel grades have kinetics similar to 2205 steel in regard to these precipitates. Sigma and chi phases precipitation occurs at higher temperatures [22]. Super duplex grades that are more highly alloyed in chromium, molybdenum, and nickel will have more rapid sigma and chi kinetics than 2205 (Figure 2) [23].

Figure 3 shows the TTT diagram with plotted curves indicating the beginning of structural transformations in the form of precipitation of secondary phases. More practical to use are TTT charts with marked curves representing a decrease of toughness by 50% measured by impact toughness testing on Charpy V specimens. An example of such a chart is shown in Figure 3. The embrittlement threshold criterion can also be used, which in most standards is set at 27 or 40 J.

Although numerous research studies describing precipitation phenomena in duplex stainless steels have been already presented [25–30] there is still no clear evidence regarding the maximum operating temperature of the steel, nor the temperature-time-microstructure relationships that determine its mechanical properties and corrosion resistance.

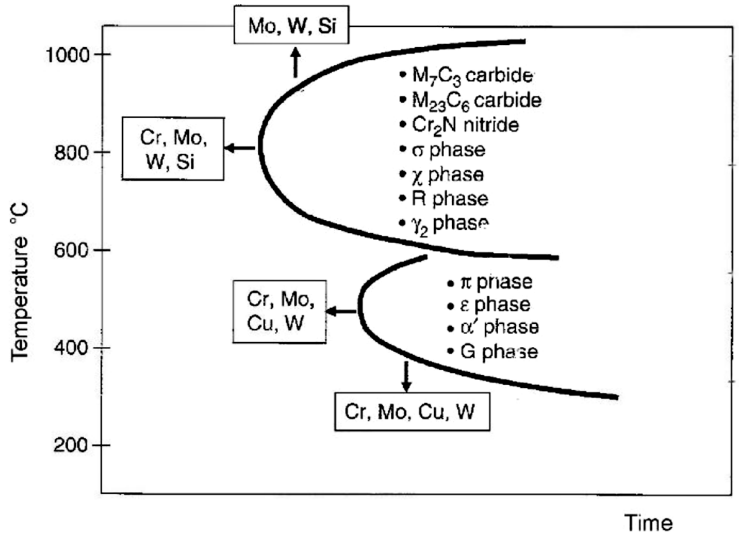

Figure 1. Schematic TTP diagram for secondary phases in duplex stainless steels [21]

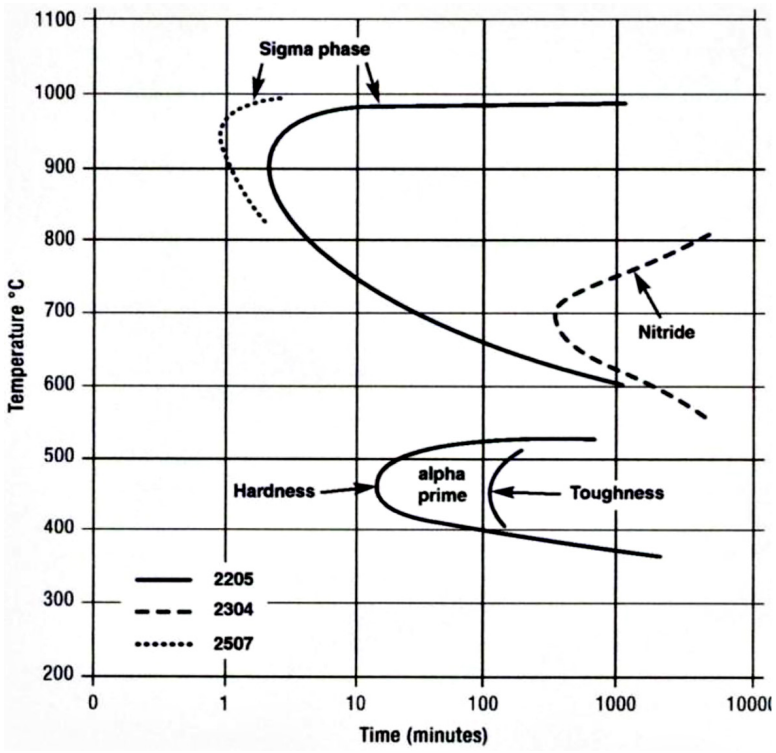

Figure 2. Isothermal precipitation diagram for duplex stainless steels, annealed at 1050 °C [23]

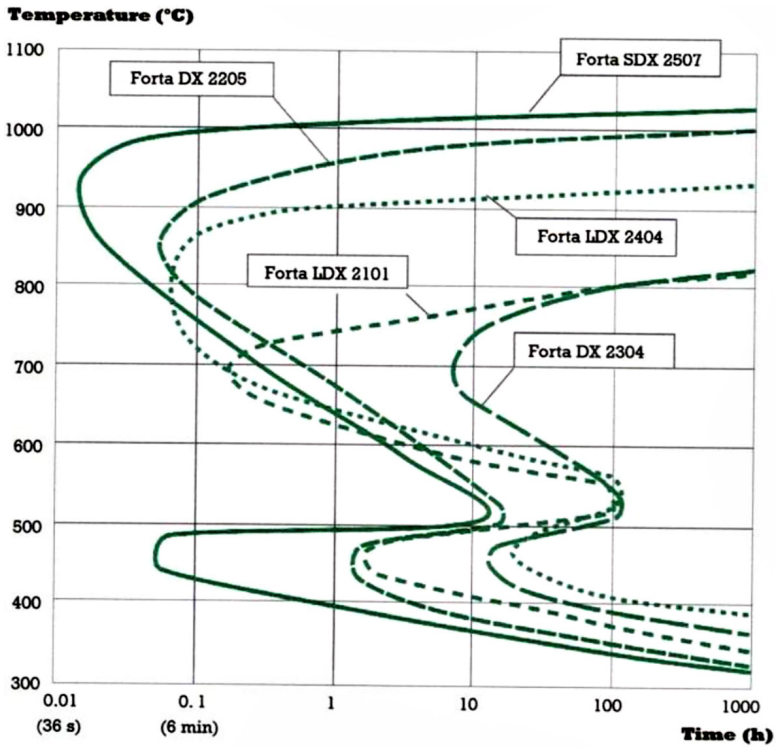

Figure 3. Temperature-time-transformation (TTT) diagram for duplex stainless steels [24]

An attempt to present such relationships for standard 2205 duplex and 2507 super duplex steels was presented in publication [31]. Currently, a group of lean duplex steels (LDX) with a depleted chemical composition has appeared on the market [20, 32–34]. Compared to the classic 2205 duplex, LDX steels do not contain a high molybdenum content, have less nickel and more

nitrogen in in chemical composition [35]. Due to its low molybdenum and high nitrogen content, UNS S32101 stainless steel is less susceptible to the formation of deleterious sigma (σ) and chi (χ) phases during heat treatment within the critical temperature range of 700–900 °C, compared to other duplex stainless steels (2205 or 2507). These phases develop only after prolonged ageing, whereas less harmful phases, such as nitrides (Cr_2N) and carbides, are more commonly observed. The balanced nitrogen content also promotes a higher austenite reformation rate [36]. LDX steels have been developed to provide higher strength alternative to 304L and 316L austenitic steels, similar corrosion resistance to 316L steel at lower cost.

Although the phenomenon of changes in the service properties of lean duplex stainless steels due to thermal cycling is well known, it has been addressed in only a few publications, which analyzed the effects of different thermal conditions on microstructural evolution, precipitation processes, and their influence on the mechanical, plastic, and corrosion-resistant properties, and susceptibility to hydrogen embrittlement of the alloy [37–44]. This further underscores the need for research in this area.

The aim of the study was to demonstrate changes in the microstructure and mechanical properties of LDX steel as a result of the impact of secondary thermal cycles and to compare the intensity of these changes to the standard duplex steel group type 2205 and the super duplex steel group. The results of the studies of 2205 duplex and 2507 super duplex steels were taken from previous studies described in [45]. The comparison of impact energy and phase stability of samples annealed at different times and temperatures aims to determine the maximum working temperature of this group of steels.

MATERIALS AND METHODS

Tests were conducted on LDX 2101 (S32101) steel. The specimens were obtained from plate 12 mm in thickness delivered after solution annealing treatment at 1050 °C. The nominal chemical composition and control analysis results of LDX 2101 steel are presented in Table 1. Additionally, this table shows the chemical compositions of duplex steel types 2205 and 2507, which have been previously studied, and the results of these studies are compared in this article. No deviations in the chemical composition of these steels in relation to the requirements of the standards were found. It is worth paying attention to the difference in the PREN parameter of the tested steels, which indicates a large difference in resistance to pitting corrosion.

Sections were cut from the LDX 2101 steel plate for the preparation of impact specimens and for metallographic examination. The sections were subjected to heat treatment. Ageing treatments were performed by isothermal holding in the vacuum furnace at temperatures from 500 to 900 °C in the time 60, 600 and 6000 minutes before water quenching. Time intervals were assumed within the limits of the greatest intensity of microstructural changes in lean duplex steel. The list of samples and their designations are shown in Table 2.

Table 2. Heat treatment conditions of samples and their designations

Temp.	Time		
	60 min.	600 min.	6000 min
500°C	5.2	5.3	5.4
600°C	6.2	6.3	6.4
700°C	7.2	7.3	7.4
800°C	8.2	8.3	8.4
900°C	9.2	9.3	9.4

Table 1. Chemical composition of tested duplex stainless steels

Duplex steel		Chemical composition, wt. %						PREN %
		C	Mn	Cr	Ni	Mo	N	
2101 S32101	Nominal	0.03	4.5	21.0	1.5	0.3	0.22	26
	Tested	0.030	5.43	21.6	1.55	0.36	0.21	
2205 S31803	Nominal	0.03	1.0	22.0	5.0	3.0	0.13	34
	Tested	0.017	1.50	21.9	5.7	3.0	0.17	
2507 S32550	Nominal	0.03	0.8	25.0	7.0	3.6	0.27	>41
	Tested	0.030	0.87	25.1	5.8	3.5	0.29	

Note: PREN =%Cr + 3.3(%Mo + 0.5x%W) + 16x%N.

Metallographic examinations were conducted using a light microscope on samples etched with with Beraha's reagent: 200 ml HCl, 1000 ml H_2O + 1 g $K_2S_2O_5$. The reagent etches the duplex steel structure, revealing ferrite as a dark (brown) phase and austenite as a light phase. The impact of heat treatment was assessed by visualizing microstructural changes, while quantitative assessment was performed using magnetic measurements of ferrite content in the microstructure. Detailed quantitative studies of the share of secondary phases (α', σ, γ_2) precipitated as a result of thermal cycles have not been presented because it is beyond the scope of this study. Magnetic measurements to determine the volume fraction of the ferrite phase were carried out using a Fischer FMP30 feritscope. For ferrite content measurement, the accuracy is within ± 5% of the standard's measurement when tested. Hardness measurements were performed using the Vickers method with a load of 98.1 N (HV10). Charpy V impact tests were performed according to the PN-EN ISO 148-1:2017-02 standard at room temperature (20 °C). The full-size (10 × 10 mm) specimens were taken in the longitudinal direction of the plate. Three samples were tested for each heat treatment condition.

RESULTS

Microstructure

The revealed microstructures of LDX 2101 steel are shown in Figure 4. This figure shows the microstructures of samples annealed for the

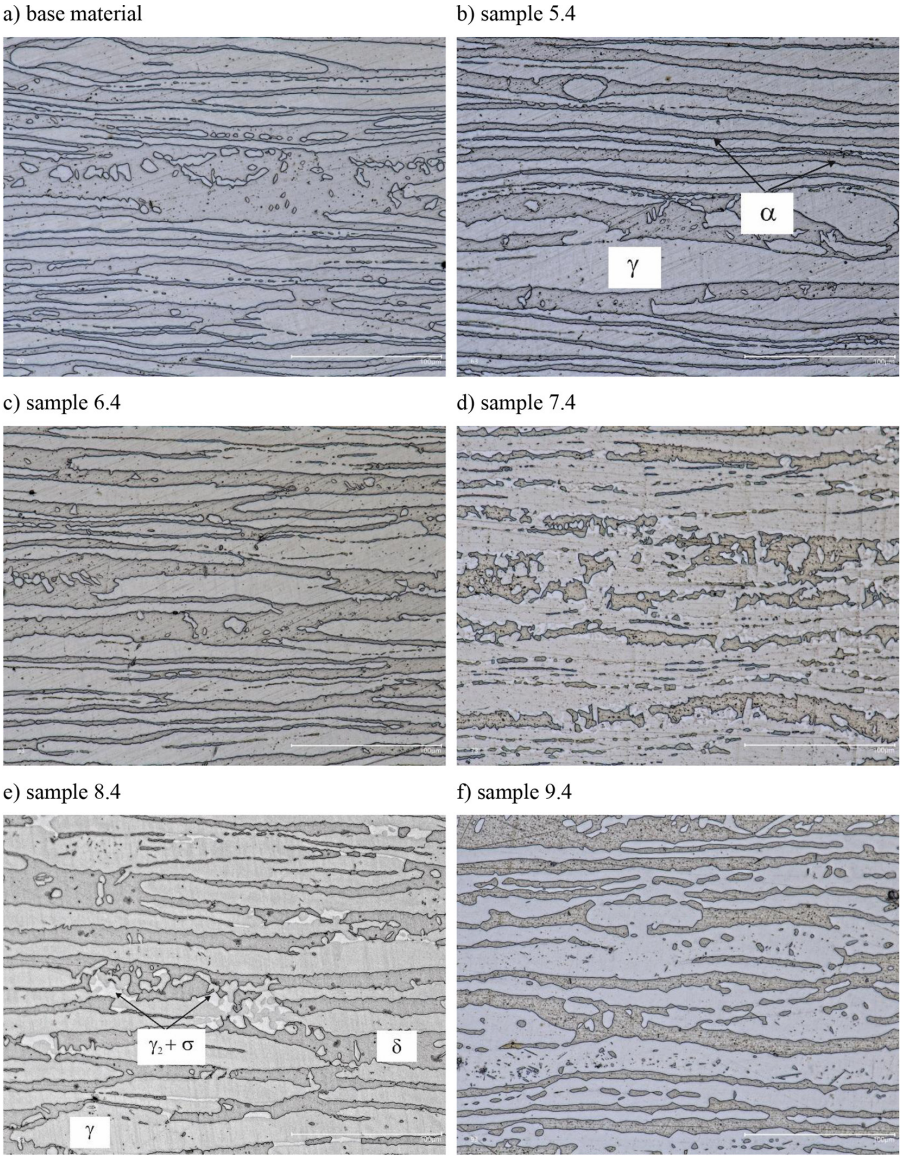

Figure 4. Microstructure of LDX 2101 steel samples after ageing at 500–900 °C for 6000 minutes

longest time (6000 min), where the most advanced changes occurred.

In the received condition, the microstructure of LDX 2101 steel had a two-phase microstructure with characteristic elongated austenite and ferrite fields aligned in the direction of deformation during rolling. The microstructure of this steel is characterized by significantly finer grain size compared to the microstructure of 2205 and 2507 duplex steels. For this reason, the magnification of the images in Figure 4 is approximately 1000x. Grain boundaries of these phases are not visible within the ferrite and austenite fields. The annealing process at temperatures of 500 and 600 °C, even after 100 hours, did not cause visible changes in the steel microstructure. Under light microscopy observation, no intermetallic phase precipitation was observed, although the formation of the α' phase was expected. Significant changes in the microstructure were observed after annealing at 700 °C. The ferrite phase content decreased significantly. A new phase appeared, visible as bright areas adjacent to the ferrite fields (Figure 4d). The phase composition of these areas can be described as a mixture of secondary austenite γ_2 and intermetallic phases, mainly σ phase. A detailed analysis of the morphology of these areas is beyond the scope of this study.

The formation of secondary austenite γ_2 can occur in two ways: as a result of a diffusion reaction and as a result of a eutectoid transformation. These are independent precipitation processes occurring in parallel, and both are related to transformations in the ferritic phase. The s phase first forms at the ferrite grain boundary or the δ/γ interface. After longer annealing times, the s phase formed as a result of a eutectoid reaction.

$$\delta \rightarrow \sigma + \gamma_2$$

At temperatures of 850–950 °C, direct transformation of ferrite to the σ phase is possible without the formation of secondary austenite. In this case, the chemical composition of the σ phase is similar to that of ferrite, but such a mechanism for σ phase formation was not observed in these studies.

It is known that the phases present in duplex stainless steel microstructures have different magnetic properties. The ferrite phase is ferromagnetic, while austenite and chromium nitride are paramagnetic, sigma and α' are nonmagnetic phases [46, 47]. Therefore, a quantitative assessment of the dynamics of phase transformations in the tested LDX 2101 steel was performed by examining the ferrite content in the microstructure. Figure 5 presents changes in the ferrite phase content in the steel microstructure depending on the ageing temperature and time. A clearly visible reduction in the ferrite content in the steel microstructure is observed during ageing at 700 °C. This confirms earlier observations from metallographic studies.

Mechanical properties

The as-delivered hardness of the steel after solution heat treatment was approximately 230 HV. The changes in the steel's hardness after ageing are shown in Figures 6 and 7. The plots show the average hardness values from at least three measurements. No significant differences in hardness were observed compared to the hardness of the base material. Ageing at 500 °C increased the steel's hardness the most, to 285 HV. This is likely due to the precipitation of the α' phase in the steel's microstructure. Ageing at 600, 800, and 900 °C at different times had virtually no effect on the hardness of the steel. During ageing at 700 °C, an increase in hardness was observed after 6000 minutes of treatment, to 264 HV10.

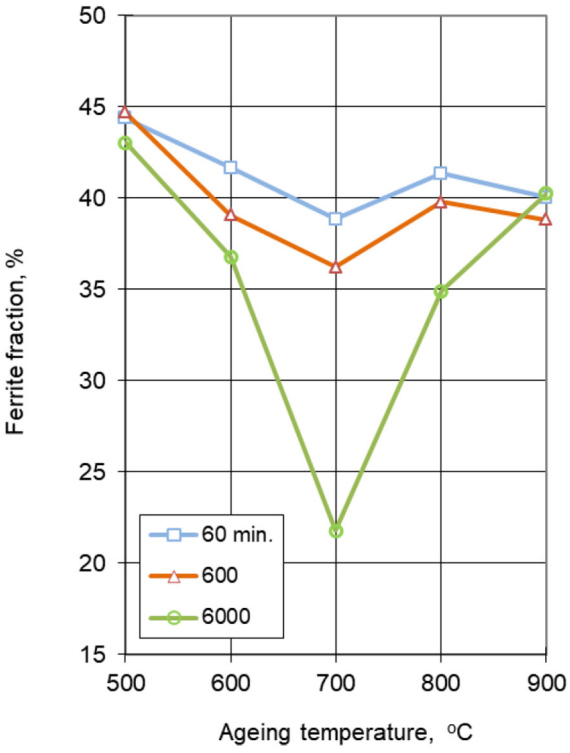

Figure 5. Ferrite content in the microstructure of LDX 2101 steel after ageing at 500–900 °C for 60, 600, 6000 min

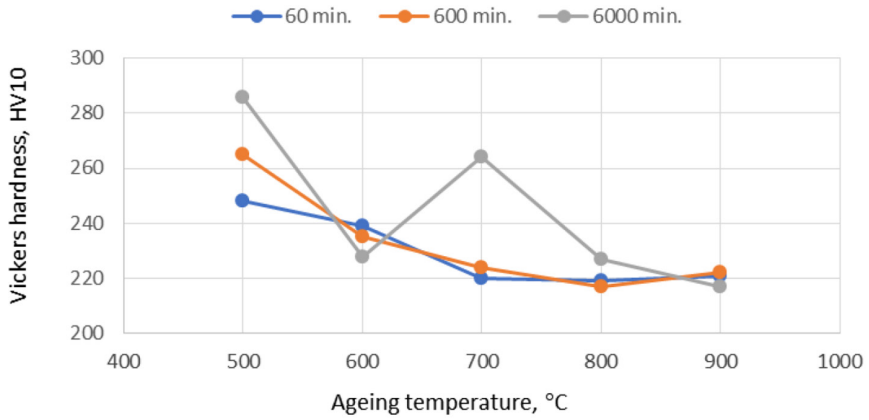

Figure 6. The influence of ageing temperature at 60, 600, and 6000 min on the hardness changes of LDX 2101 steel

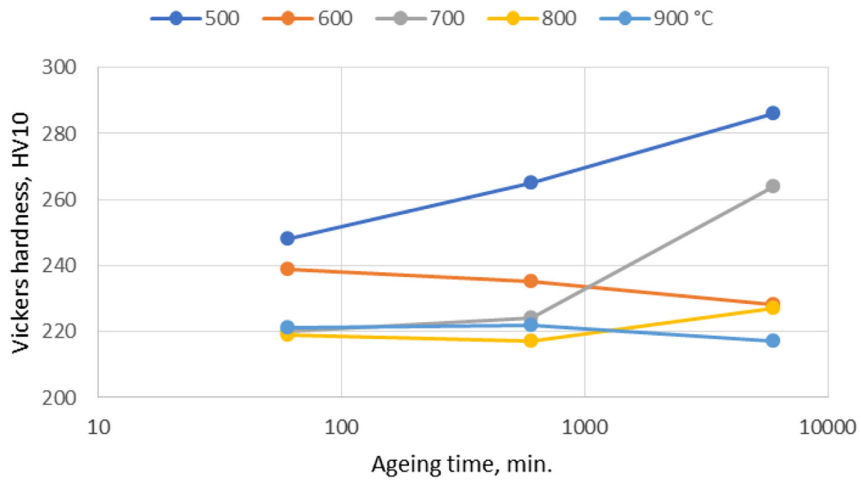

Figure 7. The influence of ageing time in the temperature range of 500–900 °C on the hardness changes of LDX 2101 steel

In the as-delivered condition (after solution heat treatment), the impact toughness of the steel was above 300 J. The impact test results of the aged samples (average values) are presented in the graphs in Figures 8 and 9.

Samples aged at 500 and 600 °C exhibited a nearly monotonic loss of impact toughness with annealing time. The greatest decrease in impact toughness was observed for samples aged at 700 °C, where after annealing for 100 hours, the impact energy decreased tenfold (to 27 J). Ageing at 700 °C also caused a significant decrease in impact energy, but only after longer ageing times, exceeding 10 hours, while ageing at 900 °C only slightly reduced impact energy.

The fracture behavior of the impact samples was assessed using macroscopic metallographic examination. Figure 10 shows the fracture behavior of the untreated material, and Figure 11 compares the fracture behavior of samples aged for 60 minutes and 6000 minutes in the temperature range of 500–900 °C. The fracture images allow for a qualitative assessment of the plasticity of the tested samples [48, 49]. As delivered, the fracture area of the samples exhibited a typical ductile behavior with significant plastic deformation of the edges. Similar fracture behavior was observed in samples aged for 60 minutes at temperatures of 600, 700, 800, and 900 °C. Only the fracture behavior of the sample aged at 500 °C exhibited brittle characteristics. Prolonged ageing of LDX 2101 duplex steel for 6000 minutes resulted in a change in the fracture behavior of the samples from ductile to brittle with a low degree of plastic deformation. The exception were samples aged at 900 °C where the ductile nature of the fractures was retained for all heat treatment times.

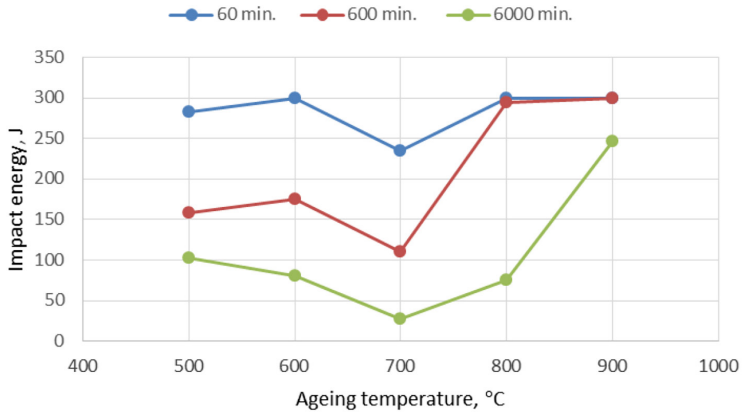

Figure 8. Effect of ageing temperature at 60, 600, and 6000 min on impact energy changes of LDX 2101 steel

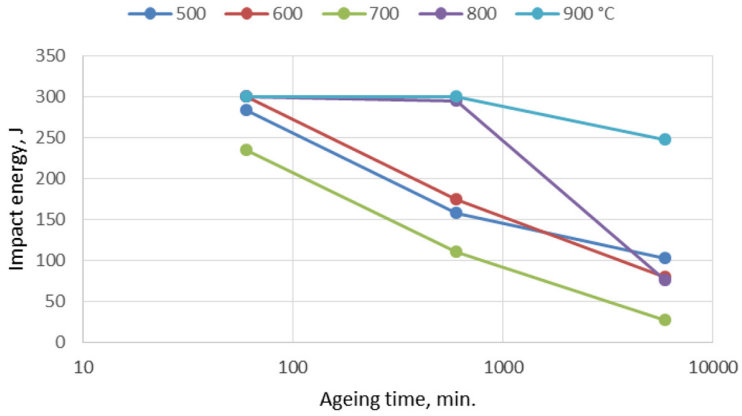

Figure 9. Influence of ageing time in the temperature range of 500–900 °C on the impact energy changes of LDX 2101 steel

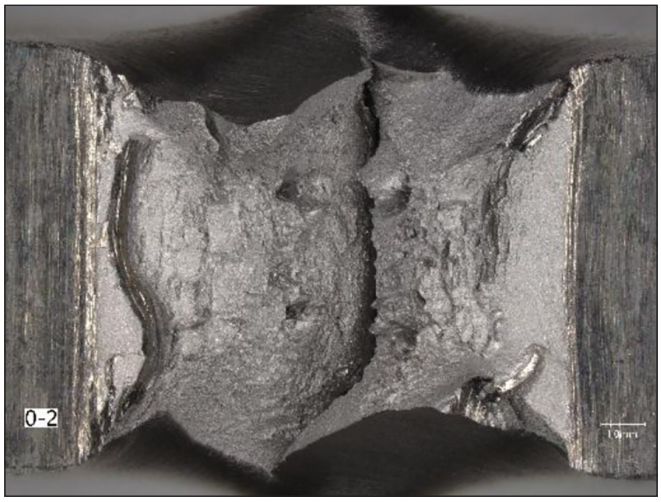

Figure 10. Fracture area of the impact test sample made of the base material

DISCUSSION

The changes in the impact toughness of LDX 2101 steel samples after ageing were dependent on microstructural transformations. Microstructural transformations associated with the precipitation of the α' phase were responsible for the reduction in impact energy after ageing at temperatures of 500 and 600 °C. The presence of this phase was not detected in metallographic

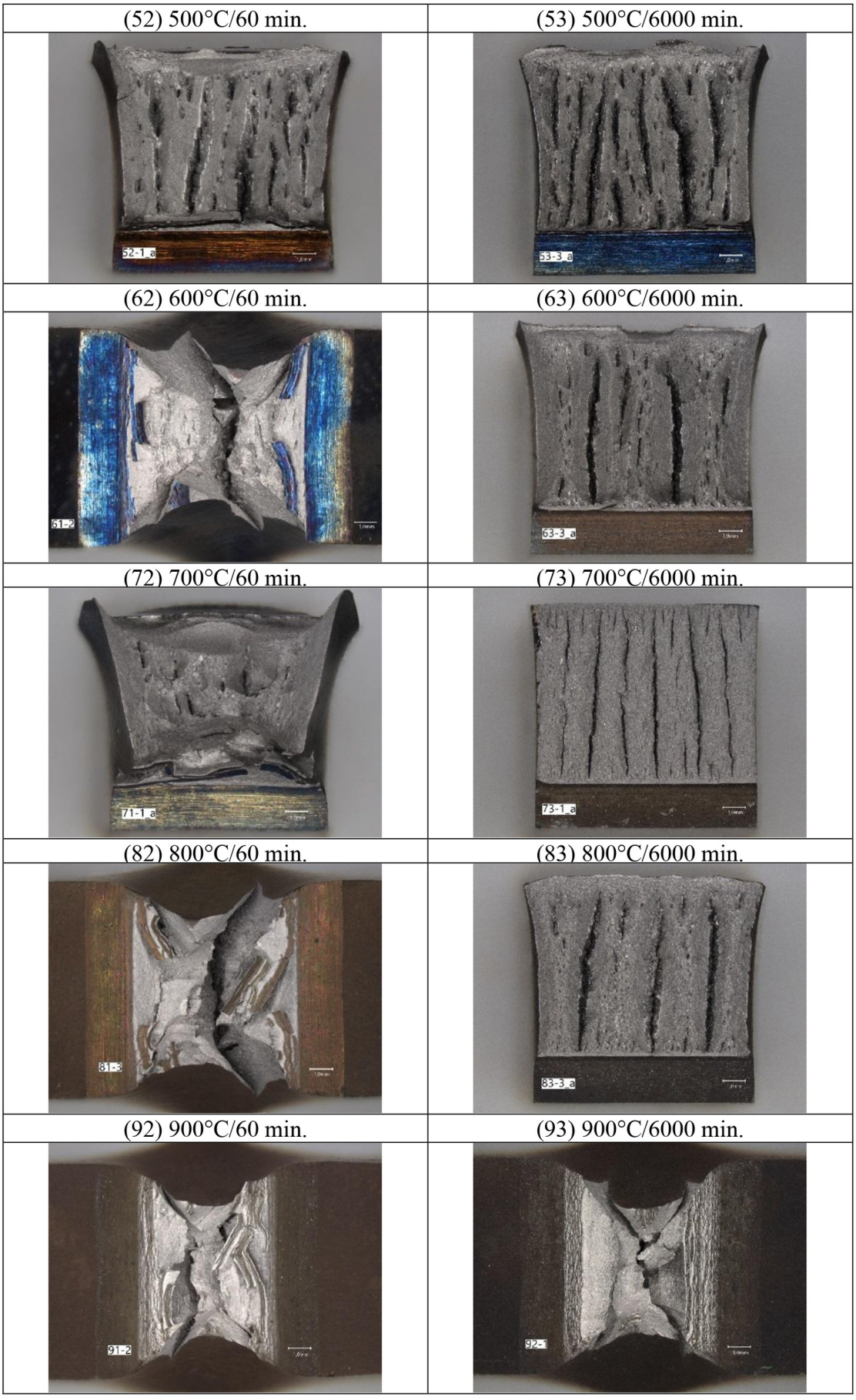

Figure 11. Fracture areas of impact samples after ageing at temperatures of 500–900 °C for 60 and 600 min

studies due to the fine nature of its precipitates. The presence of secondary phases σ and γ_2 was responsible for the decrease in impact toughness of the steel after ageing at 700 and 800 °C [16, 50]. The volume fraction of these phases in the microstructure determined the dynamics of the impact toughness decrease. Ageing at 700 °C led to the highest fraction of secondary σ and γ_2 phases, which directly contributed to the reduction in the steel's impact toughness due to embrittlement of the ferritic matrix. In contrast, ageing the samples at 900 °C for up to 6000 minutes did not result in precipitation or noticeable microstructural changes, and consequently, the impact toughness remained high, indicating the thermal stability of the steel under service conditions at elevated temperatures. The presented changes in impact toughness correlate well with the temperature-time-transformation diagram for LDX 2101 duplex stainless steel (Figure 3).

In industrial practice, it is extremely important to determine the maximum operating temperature of duplex steel in continuous operation and the safe conditions for short-term heating of steel in various technological processes, e.g. during welding or hot straightening [51].

Previously conducted tests [45] for 2205 and 2507 duplex steels showed their tendency to brittleness, especially after exposure to temperatures above 700 °C. The changes in ferrite content after various ageing treatment conditions for 2205 and 2507 duplex steels are shown in Figures 12a and 12b. The decrease in ferrite fraction is most emphasized at 800 °C where almost all ferrite content can be transformed into other phases, mainly σ and γ_2. Comparison of tendency to decomposition of ferrite structure for both tested steels show similar behavior for short exposure times (6 min). Longer exposure times results in instability of ferrite and greater reduction of this phase in 2507 super duplex steel microstructure. The amount of ferrite is higher after ageing at 900 °C than at 800 °C due to direct transformation ferrite into σ phase at higher temperatures. A comparison of the graphs in Figure 12 and Figure 5 reveals significantly less advanced ferrite transformation in the microstructure of LDX 2101 steel after ageing at temperatures above 700 °C. This obviously affects the steel's plasticity.

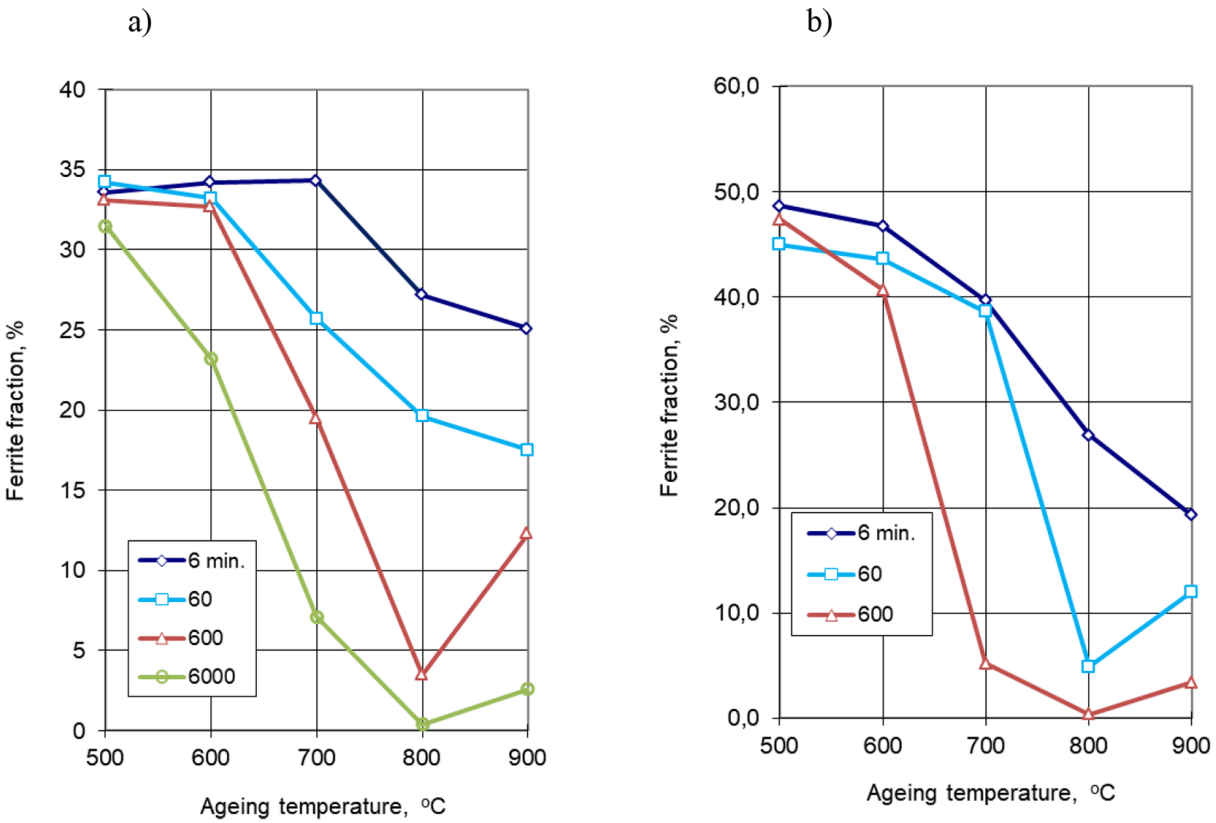

Figure 12. Changes of ferrite fraction as a function of ageing conditions for (a) 2205 duplex steel and (b) 2507 duplex steel [45]

Figure 13 compares the impact energy for 2101, 2205, and 2507 duplex steels after ageing in the temperature range of 500–900 °C. Analysis of the graphs in Figure 13 indicates that the upper temperature limit for duplex stainless steel service is controlled by α' formation. It is worth emphasizing that the loss of ductility after ageing at 500 °C most affects LDX 2101 steel, while

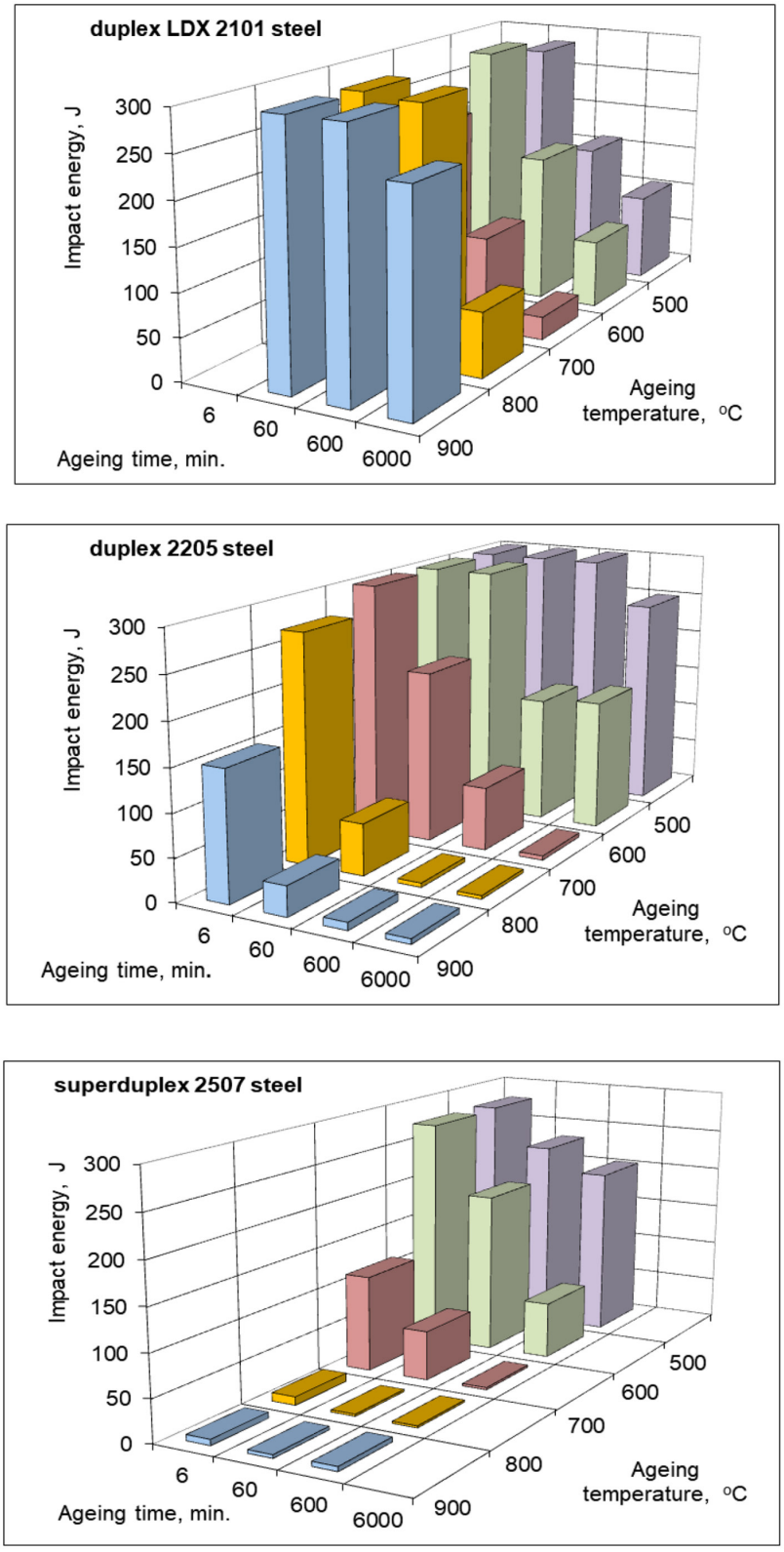

Figure 13. The influence of ageing time and temperature on impact energy of (a) 2101, (b) 2205 [45] and (c) 2507 [45] duplex stainless steels

ageing at higher temperatures – above 700 °C – limits the ductility of 2205 and 2507 steels to a much greater extent.

CONCLUSIONS

This work concerns the influence of ageing heat treatment in the range of 500–900 °C on the microstructure and mechanical properties of 2101 lean duplex stainless steel, with particular emphasis on impact toughness, and includes a comparison with 2205 and 2507 duplex steel grades. Based on the results of microstructural observations, hardness measurements, and impact toughness tests, the following conclusions were drawn:

1. Isothermal heat treatment of 2101 LDX steel in the temperature range of 500–800 °C caused destabilization of the ferritic phase and precipitation of the intermetallic phases α' at lower temperatures and σ and γ_2 phases at higher temperatures >700 °C. Ageing at 900 °C did not cause significant changes in the steel's microstructure.
2. The lowest stability of the ferritic phase in 2101 steel was observed during ageing at 700 °C.
3. Ageing at 500 °C increased the hardness of 2101 duplex steel the most, while ageing at temperatures of 600, 800, and 900 °C at different times had no significant effect on hardness changes. A hardness increase was observed after long-term annealing at 700 °C.
4. Secondary thermal cycles caused a reduction in the impact toughness of duplex 2101 steel. The greatest reduction in impact toughness was observed for samples aged at 700 °C, while ageing at 900 °C had no significant effect on the steel's ductility.
5. Comparing the ferritic phase content in the microstructure of the three duplex steels after ageing reveals a much higher stability of this phase in 2101 steel compared to 2205 and 2507 steels.
6. The three duplex steels tested showed varying degrees of embrittlement after ageing. At low ageing temperatures (500 °C), the smallest reduction in impact toughness was observed in 2205 steel, while the largest reduction was observed in 2101 steel. At higher ageing temperatures above 700 °C, the impact toughness reduction in 2101 steel was the smallest.
7. Further research should focus on the quantitative analysis of microstructure evolution in duplex steel after exposure to secondary thermal cycles, in order to provide a more comprehensive understanding of the relationships between thermal history, microstructural changes, and the resulting mechanical and corrosion-resistant properties of lean duplex stainless steels.

REFERENCES

1. Łastowska O, Starosta R, Jabłońska M, Kubit A. Exploring the potential application of an innovative post-weld finishing method in butt-welded joints of stainless steels and aluminum alloys. Materials 2024;17:1780. https://doi.org/10.3390/ma17081780
2. Szala M, Beer-Lech K, Walczak M. A study on the corrosion of stainless steel floor drains in an indoor swimming pool. Engineering Failure Analysis 2017;77:31–38. https://doi.org/10.1016/j.engfailanal.2017.02.014
3. Kumar A, Singhal A, Sirohi S, et al Pulsed current GTAW Inconel 625/AISI 304 L steel dissimilar joint: Microstructure and mechanical properties. Journal of Constructional Steel Research 2025;231:109602. https://doi.org/10.1016/j.jcsr.2025.109602
4. Szewczyk A, Jarska R, Rogalski G Effect of heat input on distortion and morphology of tungsten inert gas welded joints in AISI 304L stainless steel. Adv Sci Technol Res J 2025;19:92–104. https://doi.org/10.12913/22998624/205997
5. Henzler W, Szala M, Pałka T, et al Comparison of cavitation erosion of NiCrBSi and AISI 316L coatings deposited by powder plasma transferred Arc welding. Acta Polytech 2025;65:282–287. https://doi.org/10.14311/AP.2025.65.0282
6. Bucior M, Kluz R, Trzepieciński T, et al (2022) The effect of shot peening on residual stress and surface roughness of AMS 5504 stainless steel joints welded using the TIG method. Materials 15:8835. https://doi.org/10.3390/ma15248835
7. Quintão BM, Correa EO, Oliveira LA, et al. Avaliação da Influência do Aporte Térmico na Microestrutura da Zona Afetada pelo Calor (ZAC) de Juntas Soldadas do Aço Inoxidável ENDUR 300. Soldag insp 2024;29:e2905. https://doi.org/10.1590/0104-9224/si29.05
8. Köse C, Mutu HB, Doğan F. Effect of post weld heat treatment and filler wire on mechanical properties and microstructure of tungsten inert gas welded AISI 2507 super duplex stainless steel. J of Materi Eng and Perform 2025;34:22340–22354. https://doi.org/10.1007/s11665-025-11611-w
9. Vacchi GS, Magalhães DCC, Filho AAM, et al. Microstructural evolution and localized corrosion

behavior of friction stir welded super duplex UNS S32760 in chloride-containing environments. Journal of Materials Research and Technology 2025;36:481–499. https://doi.org/10.1016/j.jmrt.2025.03.042

10. Łabanowski J, Fydrych D, Rogalski G, Samson K. Underwater Welding of Duplex Stainless Steel. SSP 2011;183:101–106. https://doi.org/10.4028/www.scientific.net/SSP.183.101
11. Sun J, Wu C, Han Y, et al. Influence of Solution Annealing Temperature on the Microstructure, Mechanical Properties, and Corrosion Resistance of a Lean Duplex Stainless Steel Fe-0.02C-20Cr-6Mn-1Ni-0.2N-0.35Si. J of Materi Eng and Perform 2025;34:16091–16102. https://doi.org/10.1007/s11665-024-10268-1
12. Assumpção RF, Sicupira DC, Santos DB. Corrosion behavior of a 2304 lean duplex stainless steel cold-rolled and short-term annealed at different temperatures. Matéria (Rio J) 2023;28:e20230026. https://doi.org/10.1590/1517-7076-rmat-2023-0026
13. Landowski M, Simon S, Breznay C, et al. Effects of preheating on laser beam-welded NSSC 2120 lean duplex steel. International Journal of Advanced Manufacturing Technology 2024;130:1039–1074. https://doi.org/10.1007/s00170-023-12840-w
14. Maurya AK, Pandey SM, Chhibber R, et al. Corrosion performance of super duplex stainless steel and pipeline steel dissimilar welded joints: a comprehensive investigation for marine structures. Int J Adv Manuf Technol 2024;135:1009–1033. https://doi.org/10.1007/s00170-024-14596-3
15. Świerczyńska A, Łabanowski J, Michalska J, Fydrych D. Corrosion behavior of hydrogen charged super duplex stainless steel welded joints. Materials & Corrosion 2017;68:1037–1045. https://doi.org/10.1002/maco.201709418
16. Silva J, Silva E, Sampaio A, et al. Detecting the sigma phase in duplex stainless steel by magnetic noise and first harmonic analysis. Materials 2024;17:4561. https://doi.org/10.3390/ma17184561
17. Baghdadchi A, Thuvander M, Wessman S, et al. Effect of Ni content on 475 °C embrittlement of directed energy deposited duplex stainless steel using a laser beam and wire feedstock. Materialia 2024;36:102155. https://doi.org/10.1016/j.mtla.2024.102155
18. Yamada K, Osuki T, Ogawa K, et al. Effects of Mo and Cu contents on sigma phase precipitation in 25Cr-5Ni-Mo-Cu-1Mn-0.18N duplex stainless steel. ISIJ Int 2023;63:143–149. https://doi.org/10.2355/isijinternational.ISIJINT-2022-361
19. Zhang Y, Liu Z, Jin M, Song S. Effects of nitrogen element on microstructure and pitting corrosion resistance of duplex stainless steel welded joints. Mater Res Express 2021;8:026514. https://doi.org/10.1088/2053-1591/abe42f
20. Francis R, Byrne G. Duplex Stainless Steels – https://doi.org/10.3390/met11050836
21. Charles J. The duplex stainless steels: materials to meet your needs. Publ. Les Editions de Phisique, Beaune, France 1991.
22. Deng B, Wang Z, Jiang Y, et al. Effect of thermal cycles on the corrosion and mechanical properties of UNS S31803 duplex stainless steel. Corrosion Science 2009;51:2969–2975. https://doi.org/10.1016/j.corsci.2009.08.015
23. Practical guidelines for the fabrication duplex stainless steels 2014.
24. Limach-Malyar N, Jonsson J.Y, Tigerstrand C. What is the maximum operating temperature for duplex stainless steel? Stainless Steel World 2022.
25. Tuz L. An Evaluation of the Microstructure and Hardness of Co-Rich PTA Overlays on a Duplex Steel Substrate. Coatings 2025;15:69. https://doi.org/10.3390/coatings15010069
26. Ogawa K, Yamada K, Seki A. Modelling of nitride precipitation during isothermal heating after rapidly cooled from high temperature in duplex stainless steel. ISIJ Int 2022;62:1725–1730. https://doi.org/10.2355/isijinternational.ISIJINT-2022-113
27. Cojocaru EM, Raducanu D, Nocivin A, Cojocaru VD. Influence of ageing treatment temperature and duration on σ-phase precipitation and mechanical properties of UNS S32750 SDSS alloy. Journal of Advanced Research 2021;30:53–61. https://doi.org/10.1016/j.jare.2020.11.005
28. Orlowska M, Pancikiewicz K, Swierczynska A, Landowski M. Kinetics of intermetallic phase precipitation in manual metal arc welded duplex stainless steels. Materials 2023;16. https://doi.org/10.3390/ma16247628
29. Kemény DM, Sándor B, Varbai B, Katula LT. The Effects of ArC voltage and shielding gas type on the microstructure of wire ArC additively manufactured 2209 duplex stainless steel. Advances in Materials Science 2023;23:62–82. https://doi.org/10.2478/adms-2023-0023
30. Çelik BE, Talaş Ş. Mechanical Properties of UNS S31803 (2205) Duplex SS welds deposited with GTAW and SMAW methods. Soldag insp 2024;29:e2913. https://doi.org/10.1590/0104-9224/si29.13
31. Chen TH, Weng KL, Yang JR. The effect of high-temperature exposure on the microstructural stability and toughness property in a 2205 duplex stainless steel. Materials Science and Engineering: A 2002;338:259–270. https://doi.org/10.1016/S0921-5093(02)00093-X
32. Han Y, Liu Z-H, Wu C-B, et al. A short review on the role of alloying elements in duplex stainless steels. Tungsten 2023;5:419–439. https://doi.org/10.1007/s42864-022-00168-z

33. Yu X, Zhu B-Y, Bu Y, et al. Comparative studies on mechanical properties of novel lean duplex stainless steel S32001. Construction and Building Materials 2025;489:142065. https://doi.org/10.1016/j.conbuildmat.2025.142065
34. Pandey C, Thakare J, Taraphdar P, et al. Characterization of the soft zone in dissimilar welds joint of 2.25Cr-1Mo and lean duplex LDX2101 steel. Fusion Engineering and Design 2021;163. https://doi.org/10.1016/j.fusengdes.2020.112147
35. Cho Y, Kim T, Kim J. Effects of material property and thickness on block shear strength in lean duplex stainless steel welded connections. Advances in Structural Engineering 2023;26:2709–2732. https://doi.org/10.1177/13694332231199533
36. Gudikandula S, Kumar A, Dandekar TR, et al. Correlation of heat treatment and welding processes with microstructure, mechanical properties and corrosion behaviour of lean duplex stainless steels: a review. Sādhanā 2025;50:32. https://doi.org/10.1007/s12046-025-02693-2
37. Assumpçao R, de Sousa M, da Silva L, et al. Effect of low aging temperature and reversion of α′-martensite on the fracture behavior of a 2304 lean duplex stainless steel. Metallography Microstructure and Analysis 2023;12:528–544. https://doi.org/10.1007/s13632-023-00968-w
38. Dandekar T, Kumar A, Khatirkar R, et al. Effect of isothermal aging at 750 °C on microstructure and mechanical properties of UNS S32101 lean duplex stainless steel. Materials today communications 2021;29. https://doi.org/10.1016/j.mtcomm.2021.102753
39. Zhang X, Xiong Z, Cheng X. Effect of a novel heat treatment on the corrosion resistance of duplex stainless steel S32101. Journal of Materials Engineering and Performance. 2025. https://doi.org/10.1007/s11665-025-10728-2
40. Kauss N, Heyn A, Halle T, Rosemann P. Detection of sensitisation on aged lean duplex stainless steel with different electrochemical methods. Electrochimica Acta 2019;317:17–24. https://doi.org/10.1016/j.electacta.2019.05.081
41. Liu Z, Wu Z, Han Y, et al. Combination of high yield strength and improved ductility of 21Cr lean duplex stainless steel by tailoring cold deformation and low-temperature short-term aging. Acta Metallurgica Sinica-English Letters 2024;37:695–702. https://doi.org/10.1007/s40195-023-01626-4
42. Zhang B, Tu W, He P, et al. Mechanical properties and hydrogen embrittlement of lean duplex stainless steel 2101 with microstructure under different aging times. Materials Science and Engineering: A 2025;946:149077. https://doi.org/10.1016/j.msea.2025.149077
43. Silva R, Kugelmeier C, Martins CJ, et al. Mechanisms of intergranular corrosion and self-healing in high temperature aged lean duplex stainless steel 2404. NPJ Materials Degradation 2024;8. https://doi.org/10.1038/s41529-024-00541-y
44. Mota CFGS, Aota LS, Sandim HRZ, et al. Austenite reversion in lean duplex steel: Microstructural, dilatometric and magnetic characterization. Materials Characterization 2023;195:112509. https://doi.org/10.1016/j.matchar.2022.112509
45. Topolska S, Łabanowski J. Effect of microstructure on impact toughness of duplex and superduplex stainless steels. Journal of Achievements in Materials and Manufacturing Engineering 2009;36.
46. Noga P, Skrzekut T, Wędrychowicz M, et al. The influence of various welding methods on the microstructure and mechanical properties of 316Ti steel. Materials 2024;17:1681. https://doi.org/10.3390/ma17071681
47. Quackatz L, Westin EM, Griesche A, et al. Assessing ferrite content in duplex stainless weld metal: WRC '92 predictions vs. practical measurements. Weld World 2025;69:31–45. https://doi.org/10.1007/s40194-024-01878-3
48. Perković S, Sedmak A, Radaković Z, et al. Effect of temperature on S32750 duplex steel welded joint impact toughness. Materials 2023;16:4432. https://doi.org/10.3390/ma16124432
49. Wang B, Zhang Y, Shen X, et al. Austenite morphology and distribution dependence of impact toughness in S32101 duplex stainless steel laser welds. Metall Mater Trans A 2024;55:1183–1192. https://doi.org/10.1007/s11661-024-07314-x
50. Wang R. Precipitation of sigma phase in duplex stainless steel and recent development on its detection by electrochemical potentiokinetic reactivation: A review. Corrosion Communications 2021;2:41–54. https://doi.org/10.1016/j.corcom.2021.08.001
51. Burja J, Žužek B, Šetina Batič B. Influence of isothermal annealing in the 600 to 750 °C range on the degradation of SAF 2205 duplex stainless steel. CMD 2024;5:340–349. https://doi.org/10.3390/cmd5030014